Alleviating Dirty-window-effect in Medium Frame-Rate Binary Video Halftones

Hamood-Ur Rehman, and Brian L. Evans, *Fellow, IEEE*

***Abstract*—A video display device having a lower number of bits per pixel than that required by the video to be displayed quantizes the video prior to its display. Halftoning can perform this quantization while attempting to reduce the visibility of certain quantization artifacts. Quantization artifacts are, nevertheless, not eliminated. A temporal artifact known as dirty-window-effect can be commonly observed in medium frame-rate binary video halftones. In this paper, we propose video halftone enhancement algorithms to reduce dirty-window-effect. We assess the performance of the proposed algorithms by presenting objective measures for dirty-window-effect in the original and the improved halftone videos. The expected contributions of this paper include three medium frame-rate binary video halftone enhancement algorithms that (1) reduce dirty-window-effect under a spatial quality constraint, (2) reduce dirty-window-effect under a spatial quality constraint with reduced complexity, and (3) reduce dirty-window-effect under spatial and temporal quality constraints.**

***Index Terms*—video halftoning, temporal artifacts, dirty-window-effect.**

I. Introduction

DISPLAY devices having a relatively lower number of bits per pixel (i.e. bit-depth) cannot directly display a video having a higher bit-depth. To have the bit-depth of the video match that of the display device, bit-depth reduction must be performed on the video. Video halftoning performs this quantization while attempting to reduce the visibility of quantization artifacts. The original (full bit-depth) video is called the continuous-tone video, and the reduced bit-depth video is called the halftone video.

Video halftoning algorithms generally aim to make the halftone video perceptually as similar to the continuous-tone video as possible [1]–[7]. The goal is to reduce the visibility of quantization artifacts. Binary video halftones can have both spatial and temporal artifacts. Spatial artifacts in image halftones have received quite a bit of attention in the halftoning literature [8]–[20]. Two temporal artifacts commonly observed in medium frame-rate binary video halftones are flicker, and dirty-window-effect (DWE) [1], [21]. Flicker in binary video halftones has been discussed in [1], [3]–[6], [21]. DWE in binary video halftones has been discussed in [1], [2].

In the generation of video halftones, reduction in the visibility of one temporal artifact can sometimes lead to an increase in the visibility of another temporal artifact. The focus of this paper is on reducing the visibility of DWE in medium frame-rate (15 to 30 frames per second) binary video halftones produced from grayscale continuous-tone videos. This paper describes a portion of binary video halftone enhancement work developed in [22]. The algorithms presented in this paper are not video halftone generation algorithms. Instead, the proposed algorithms are designed to enhance a medium frame-rate binary *halftone* video that suffers from intense DWE. In the process of such enhancement of a halftone video, the availability of the corresponding continuous-tone video is still needed. To assess the results of enhancement, the objective artifact assessment measures developed in [1] are utilized.

Dirty-window-effect in medium frame-rate binary halftone videos has been described in detail in [1]. For binary video halftones, DWE refers to the temporal artifact that makes the objects look as if they were being viewed through a "dirty window." This artifact is disturbing to the viewer because it can give the perception of a pattern being laid on top of the actual video content [1]. This is why reduction of DWE is important. DWE is a local phenomenon [1]. Consider a medium frame-rate binary halftone video produced by halftoning a grayscale continuous-tone video. Each frame of the halftone video is a pattern of binary pixels. Although each pixel can only have two values, due to the averaging properties of the human visual system (HVS), a human viewer perceives each binary frame as having several gray levels. Now consider a scenario where two successive frames of the continuous-tone video differ in content in some spatial regions. This could, for example, be the case due to motion (between successive frames) in these spatial regions. If the local binary patterns between the corresponding successive halftone frames do not change "sufficiently" to reflect the change of content (in the changing spatial regions), DWE is likely to be observed. It is also possible that when viewed as static frames, each frame represents a good halftone of the corresponding continuous-tone frame. However, when viewed in sequence, due to DWE, it might seem like the video content is being viewed through a "dirty" window. Said another way, DWE is caused due to the "over-stability" of binary pixels in the temporal dimension. This excessive stability of pixels is a problem in regions where there is a change of content, due to motion for example.

To reduce DWE in a medium frame-rate binary halftone video, it is desirable for the (local) binary pixel patterns to change in spatial regions where there is any change of content [1]. If binary pixel patterns also change in regions where there is no change of content, then flicker might be observed [1], [21]. Too many changes in binary pixel values between successive halftone frames can cause perception of flicker.

In this paper, we adopt the notation introduced in [22]. The notation, as used in this paper, is described in table I. Please

H. Rehman was and B. L. Evans is with the Department of Electrical and Computer Engineering, The University of Texas at Austin, Austin, Texas, USA. B. L. Evans' e-mail: bevans@ece.utexas.edu

refer back to Table I whenever needed. We let I be the total number of frames in V_c. We also let M be the total number of pixel rows in each frame of V_c, and N be the total number of pixel columns in each frame of V_c.

The remainder of the paper is organized as follows. Section II introduces the HVS model used in this paper. Section III presents the design of the proposed algorithms. Section IV evaluates the proposed algorithms by presenting and discussing the results of video halftone enhancement on several example video sequences. Section V presents the DWE and flicker performance of halftone videos generated using some other algorithms. Finally, Section VI concludes the paper.

II. Human Visual System Model

The algorithms proposed in this paper attempt to reduce DWE without degrading the perceived spatial quality of the individual frames of the halftone video. To do so, the algorithms require a perceptual measure for the spatial quality of each halftone frame. To get this measure for the perceived quality of a halftone frame, the proposed algorithms utilize a spatial model for the HVS.

Different spatial HVS models have been tested for use in image halftoning algorithms [23]–[29]. The performance of different HVS models [30]–[33] was evaluated for direct binary search (DBS) based halftoning in [34], and it was found that Nasanen's model, which gives a low-pass approximation, produced halftones with the best subjective quality. It was earlier shown by Mitsa and Varkur [28] that for quantitative evaluation of halftoning applications, low-pass constrast sensitivity function (CSF) performs better than a bandpass CSF.

For the reasons discussed above, in this paper, the spatial characteristics of the HVS are modelled by a linear shift invariant system [35], [36], represented by a two-dimensional low-pass filter. In particular, we use Nasanen's model [32] to demonstrate the effectiveness of the proposed algorithms. Note, however, that the algorithms presented in this paper are not dependent on any particular type of HVS model. Recall that the goal of this paper is to introduce the algorithms that enhance medium frame-rate binary video halftones. We do so using a model of HVS that has been shown to work [34].

The general form of frequency response, $H_r(f_r)$, for Nasanen's model is

$$H_r(f_r) = aL^b e^{-(f_r/[c\ln(L)+d])} \tag{1}$$

where f_r is the radial spatial frequency, L is average luminance, and a, b, c, and d are constants. The unit of spatial frequency is cycles per degree.

Let p represent the point spread function of the HVS. The point spread function of the HVS is obtained from the frequency response of the HVS. Ignoring the effects of the display device, the perceived i^{th} continuous-tone frame, $\widetilde{C}_i$, is given by:

$$\widetilde{C}_i = C_i * p \tag{2}$$

where $*$ represents two-dimensional convolution.
The perceived i^{th} halftone frame, $\widetilde{D}_i$, is given by:

$$\widetilde{D}_i = D_i * p \tag{3}$$

The perceived i^{th} enhanced halftone frame, $\widetilde{DE}_i$, is given by:

$$\widetilde{DE}_i = DE_i * p \tag{4}$$

The i^{th} error frame is defined as the difference of the i^{th} continuous-tone and halftone frames. Let $E_{i,d,c}$ be the i^{th} error frame corresponding to the i^{th} halftone frame D_i. Each pixel of $E_{i,d,c}$, $E_{i,d,c}(m,n)$ is given by:

$$E_{i,d,c}(m,n) = C_i(m,n) - D_i(m,n) \tag{5}$$

The associated perceived i^{th} error frame corresponding to the i^{th} halftone frame D_i is given as:

$$\widetilde{E}_{i,d,c} = E_{i,d,c} * p \tag{6}$$

The perceived total squared error of D_i (with respect to C_i), $\widetilde{E}_{i,d,c,total}$, is defined as:

$$\widetilde{E}_{i,d,c,total} = \sum_m \sum_n \left| \widetilde{E}_{i,d,c}(m,n) \right|^2 \tag{7}$$

This is the (frame) error metric that will be used to constrain the perceptual degradation that the i^{th} halftone frame might experience as a result of reducing DWE in the halftone video.

III. Proposed Algorithms

This section discusses the development of three video halftone enhancement algorithms. These algorithms are iterative algorithms. This means that it might take more than one pass to generate the enhanced output video. The algorithms can be used to enhance medium frame-rate binary halftone videos that suffer from excessive DWE. As inputs, the enhancement algorithms require the binary halftone video to be enhanced, V_d, and the corresponding grayscale continuous-tone video, V_c. The algorithms assume no knowledge of how the input halftone video, V_d, is generated. The output of each enhancement algorithm is the enhanced video, V_{de}, with reduced DWE.

A. Algorithm I: Reducing Dirty-window-effect under Spatial Quality Constraint

In this section, we develop a method to reduce DWE. Recall that DWE is caused by "temporal overstability" of binary pixels, in (spatial) regions that change content between successive frames. The goal in DWE reduction is, then, to toggle the binary pixels values between successive frames. Generally, this would result in increased flicker.

Initially, the pixels of the output halftone video V_{de} are set to be equal to the input halftone video V_d. Then, in the process of reducing DWE, some pixels of (*initial*) V_{de} are toggled to produce the (*final*) halftone video V_{de} to be output. Recall from Table I that ψ_i denotes the *ordered* set of pixels that change, as a result of enhancement, in the output halftone frame DE_i. The order in which elements appear in this set indicates the order in which the pixels get changed. Also, recall that U_i

TABLE I
NOTATION

Symbol	Description
V_c	Continuous-tone video;
V_d	The corresponding halftone video;
V_{de}	The enhanced halftone video produced by reducing artifacts in halftone video, V_d;
C_i	The i^{th} frame of continuous-tone (original) video, V_c;
$C_i\,(m,n)$	Pixel located at m^{th} row and n^{th} column of the continuous-tone frame C_i;
$\widetilde{C}_i$	The i^{th} perceived (by a human viewer) frame of the halftone video, V_c;
$\widetilde{C}_i\,(m,n)$	Pixel located at m^{th} row and n^{th} column of the perceived continuous-tone frame $\widetilde{C}_i$;
D_i	The i^{th} frame of halftoned video, V_d;
$D_i\,(m,n)$	Pixel located at m^{th} row and n^{th} column of the halftone frame D_i;
$\widetilde{D}_i$	The i^{th} perceived (by a human viewer) frame of the halftone video, V_d;
$\widetilde{D}_i\,(m,n)$	Pixel located at m^{th} row and n^{th} column of the perceived halftone frame $\widetilde{D}_i$;
$\widetilde{E}_{i,d,c,total}$	The perceived total squared error of D_i with respect to C_i;
DE_i	The i^{th} frame of the enhanced halftone video, V_{de};
$DE_i\,(m,n)$	Pixel located at m^{th} row and n^{th} column of the enhanced halftone video DE_i;
$\widetilde{DE}_i$	The i^{th} perceived (by a human viewer) frame of the enhanced halftone video, V_{de};
$\widetilde{DE}_i\,(m,n)$	Pixel located at m^{th} row and n^{th} column of the perceived continuous-tone frame $\widetilde{DE}_i$;
$\Delta DE_{i,i-1}$	The absolute difference image for frames DE_i, DE_{i-1};
$\widetilde{E}_{i,de,c,total}$	The perceived total squared error of DE_i with respect to C_i;
ψ_i	The *ordered* set of pixels that change in DE_i as a result of enhancement;
U_i	The total number of pixels that get changed in DE_i as a result of enhancement;
ζ_i	The *ordered* set of pixel locations corresponding to pixels in ψ_i.

denotes the total number of pixels that get changed in DE_i to produce the *final* output frame DE_i. We let k index the elements of ψ_i. We also let the k^{th} pixel in the ordered set ψ_i to be denoted by $u_{i,k}$. ζ_i represents the *ordered* set of *pixel locations* corresponding to the pixels in the set ψ_i. Observe that the order of the elements of the set ζ_i depends on the order of the elements of the set ψ_i, and that k indexes the elements of ζ_i as well. We denote the k^{th} element of ζ_i by $x_{i,k}$. We can then write:

$$U_i \leq M \cdot N \tag{8}$$

$$\psi_i = \{u_{i,k} : 1 \leq k \leq U_i\} \tag{9}$$

$$|\psi_i| = U_i \tag{10}$$

$$\zeta_i = \{x_{i,k} : DE_i(x_{i,k}) \in \psi_i\} \tag{11}$$

$$|\zeta_i| = |\psi_i| \tag{12}$$

For $i > 1$, each pixel $\Delta DE_{i,i-1}(m,n)$ of the i^{th} absolute difference image, $\Delta DE_{i,i-1}$ is given by:

$$\Delta DE_{i,i-1}(m,n) = |DE_i(m,n) - DE_{i-1}(m,n)| \tag{13}$$

Thus, $\Delta DE_{i,i-1}(m,n)$ is binary valued.

Fig. 1 is a formal illustration of the enhancement algorithm used to reduce DWE. We begin by setting the output enhanced halftone video V_{de} to be equal to the input halftone video V_d. The video V_{de} is then modified frame-by-frame starting from its second frame, DE_2, and sequentially processing the rest. The first output frame, DE_1 remains unchanged (i.e. equal to the first input frame D_1). For $i \geq 2$, each final output frame DE_i gets produced by pixel-by-pixel traversing the initial output frame DE_i at those pixel locations where DE_i and DE_{i-1} have the same value. The traversed pixels locations have values that could *potentially* cause any perceived DWE. Note from Fig. 1 that we let ξ_i be the ordered set of pixel locations that have the same values between the two adjacent frames DE_i and DE_{i-1}. Let the elements of ξ_i be indexed by j. We denote the j^{th} element of ξ_i by $w_{i,j}$. Note that $w_{i,j}$ represents a pixel location vector. Said another way, if (m,n) is the spatial location whose value stays the same between the adjacent frames DE_i and DE_{i-1}, then $w_{i,j} = (m,n)$ for some value of j. Observe that $DE_i(m,n)$ could more succinctly be written as $DE_i(w_{i,j})$. Therefore,

$$\xi_i = \{w_{i,j} : DE_i(w_{i,j}) = DE_{i-1}(w_{i,j})\} \tag{14}$$

The order of elements in ξ_i depends on pixel traversal strategy during a particular scan of a frame. An example traversal strategy is raster scan order. Let us take a look at the processing of the i^{th} enhanced halftone frame. At the start of the first scan, the binary pixel $DE_i(w_{i,1})$ (of frame DE_i) is toggled. This means we are changing its value from either a "1" to a "0" or from a "0" to a "1." Let us call this change a trial change. If this trial change causes the difference in the total (squared) perceptual error between the enhanced halftone frame DE_i, and the continuous-tone frame C_i, and the total (squared) perceptual error between the original halftone frame D_i and the continuous-tone frame C_i to be lower than or equal to a certain threshold T_0, then the pixel toggle is acceptable and the changed value of this pixel is retained. Otherwise, the pixel value is changed back to what it was before the trial change (i.e. it is toggled again.). This process is carried out at each pixel location in the set ξ_i until all the pixel locations in the set ξ_i have been visited. This constitutes first complete scan of the frame. One complete scan of the i^{th} frame refers to

traversing the set of pixel locations, ξ_i, once. After completing a scan, the elements of ξ_i that represent pixel locations whose values were changed during the scan are removed from the set ξ_i. This gives us a different set ξ_i for the next possible scan.

After a complete scan of the frame DE_i, before initiating the next scan, we check whether another scan is needed or not. This is done by checking for convergence. For example, we could say that the frame DE_i has converged to its final form if the number of pixel changes in the (last) completed scan is below a certain value. Different convergence criteria could be used, however. The scan is only repeated on the enhanced frame DE_i, if the convergence criterion is not met. Note that if a scan is repeated with a different pixel traversal strategy, then the ordering of elements of the set ξ_i is accordingly changed before beginning the scan. If the convergence criterion has been satisfied, then the algorithm moves on to enhance the next frame DE_{i+1}. This process is continued until all frames have been processed in a sequence, at which point, the enhanced video V_{de} is the halftone video with reduced DWE.

To enhance the understanding of the algorithm depicted in Fig. 1, we make some observations. During any scan of the i^{th} frame DE_i, $w_{i,j}$ ($\in \xi_i$) denotes the spatial coordinates of the j^{th} pixel whose value is trial changed. $DE_i^{w_{i,j}}$ denotes the enhanced frame DE_i *after* the pixel at location $w_{i,j}$ is trial changed. The corresponding perceived error frame is given by:

$$\widetilde{E}_{i,de,c}^{w_{i,j}} = (C_i - DE_i^{w_{i,j}}) * p \tag{15}$$

The perceived total squared error of $DE_i^{w_{i,j}}$ (with respect to C_i), $\widetilde{E}_{i,de,c,total}^{w_{i,j}}$ is given by:

$$\widetilde{E}_{i,de,c,total}^{w_{i,j}} = \sum_m \sum_n \left| \widetilde{E}_{i,de,c}^{w_{i,j}}(m,n) \right|^2 \tag{16}$$

It is important to note that $\widetilde{E}_{i,de,c,total}^{w_{i,j}}$ is the total perceived error between DE_i, and C_i due to all pixel changes that have been accepted thus far, including the changes accepted in the previous scans of DE_i, as well as the *trial* change at pixel location $w_{i,j}$ ($\in \xi_i$).

The value of the threshold T_0 controls the amount of DWE reduction in the enhanced halftone video V_{de}. T_0 also controls any degradation in the spatial quality of the frame DE_i that might occur as a result of DWE reduction. A lower value of T_0 will favor a higher spatial quality of the frame at the expense of not reducing DWE as effectively. A higher value of T_0 will reduce DWE more, but could potentially result in the deterioration of the perceptual quality of individual frames. Observe from Fig. 1 that if T_0 is set to zero, the enhanced (output) frames would *theoretically* have at least as good a perceptual spatial quality (as defined by the measure of (16)) as the original (input) halftone frames. The frames could, of course, differ in how the binary pixels are spatially distributed. Using a higher value of T_0 could alleviate DWE more, but would likely degrade the frames' spatial quality more.

The DWE reduction algorithm developed in this section is computationally inefficent. To appreciate this fact, please refer to Fig. 1 to note that the evaluation of ($\widetilde{E}_{i,de,c,total}^{w_{i,j}} - \widetilde{E}_{i,d,c,total} \leq T_0$) is done for each pixel in ξ_i. For the evaluation of this expression, both $\widetilde{E}_{i,de,c,total}^{w_{i,j}}$ and $\widetilde{E}_{i,d,c,total}$ need to be computed. Of these two, $\widetilde{E}_{i,d,c,total}$ needs to be computed once per frame. However, $\widetilde{E}_{i,de,c,total}^{w_{i,j}}$ needs to be computed for each pixel trial change in the (enhanced) frame DE_i. Note from (15) and (16), that the evaluation of $\widetilde{E}_{i,de,c,total}^{w_{i,j}}$ requires a convolution operation between the error image $(C_i - DE_i^{w_{i,j}})$ and the HVS filter p. Even if a complete image convolution is not carried out to update the value of $\widetilde{E}_{i,de,c,total}^{w_{i,j}}$ to reflect the effect of trial change, its evaluation would still involve several pixels of the error image $(C_i - DE_i^{w_{i,j}})$. Thus, this operation is computationally expensive rendering the algorithm of Fig. 1 relatively inefficient computationally.

B. Algorithm II: Computationally Efficient Reduction of Dirty-window-effect under Spatial Quality Constraint

To make the idea introduced in Section III-A computationally feasible, in this section, a variant of the algorithm of Fig. 1 is developed. The resulting modified algorithm reduces DWE in a computationally more efficient manner.

It was discussed in the previous section that evaluating the effect of a trial change is computationally expensive. An efficient method to evaluate the effect of trial pixel changes has been described in [36], [37]. We would like to use that efficient evaluation of trial changes [36], [37] in our algorithm. To describe how the algorithm of this section is computationally more feasible, we introduce some more notation. Let $\Delta\widetilde{E}_{i,de,c,total}^{w_{i,j}}$ be the *change* in perceptual error that results due to the trial change in the value of the pixel at location $w_{i,j}$ in the i^{th} enhanced frame, DE_i. Let $\widetilde{E}_{i,de,c,total}^{\delta}$ be the perceptual error between DE_i and C_i before the pixel located at $w_{i,j}$ is changed for trial. Thus, $\Delta\widetilde{E}_{i,de,c,total}^{w_{i,j}}$ is:

$$\Delta\widetilde{E}_{i,de,c,total}^{w_{i,j}} = \begin{cases} \widetilde{E}_{i,de,c,total}^{w_{i,j}} - \widetilde{E}_{i,de,c,total}^{\delta} & \text{for } 2 \leq j \leq M \cdot N, \\ \widetilde{E}_{i,de,c,total}^{w_{i,j}} - \widetilde{E}_{i,d,c,total} & \text{for } j = 1. \end{cases} \tag{17}$$

Let us assume that the pixel located at $w_{i,1}$ is trial-changed. Note that, based on our notation introduced thus far, this is the first pixel location undergoing a trial change in the i^{th} frame DE_i. If we want to use the efficient method of evaluating $\Delta\widetilde{E}_{i,de,c,total}^{w_{i,1}}$, as proposed in [36], [37], we will need correlation matrices c_{pp} and $c_{p\widetilde{E}_{i,de,c}}$. These correlation matrices are given by:

$$c_{pp} = p \otimes p \tag{18}$$

$$c_{p\widetilde{E}_{i,de,c}} = p \otimes \widetilde{E}_{i,de,c} \tag{19}$$

where $\otimes$ represents the two-dimensional correlation operation. Let us define $a_i(w_{i,j})$ to be:

$$a_i(w_{i,j}) = NOT(DE_{i-1}(w_{i,j})) - DE_i(w_{i,j}) \tag{20}$$

where the logical NOT operation toggles the (binary) value of $DE_{i-1}(w_{i,j})$.

Since the pixel values are binary *and* $w_{i,j} \in \xi_i$, the value of $a_i(w_{i,j})$ will be either 1 or -1. Recall from (14), ξ_i represents

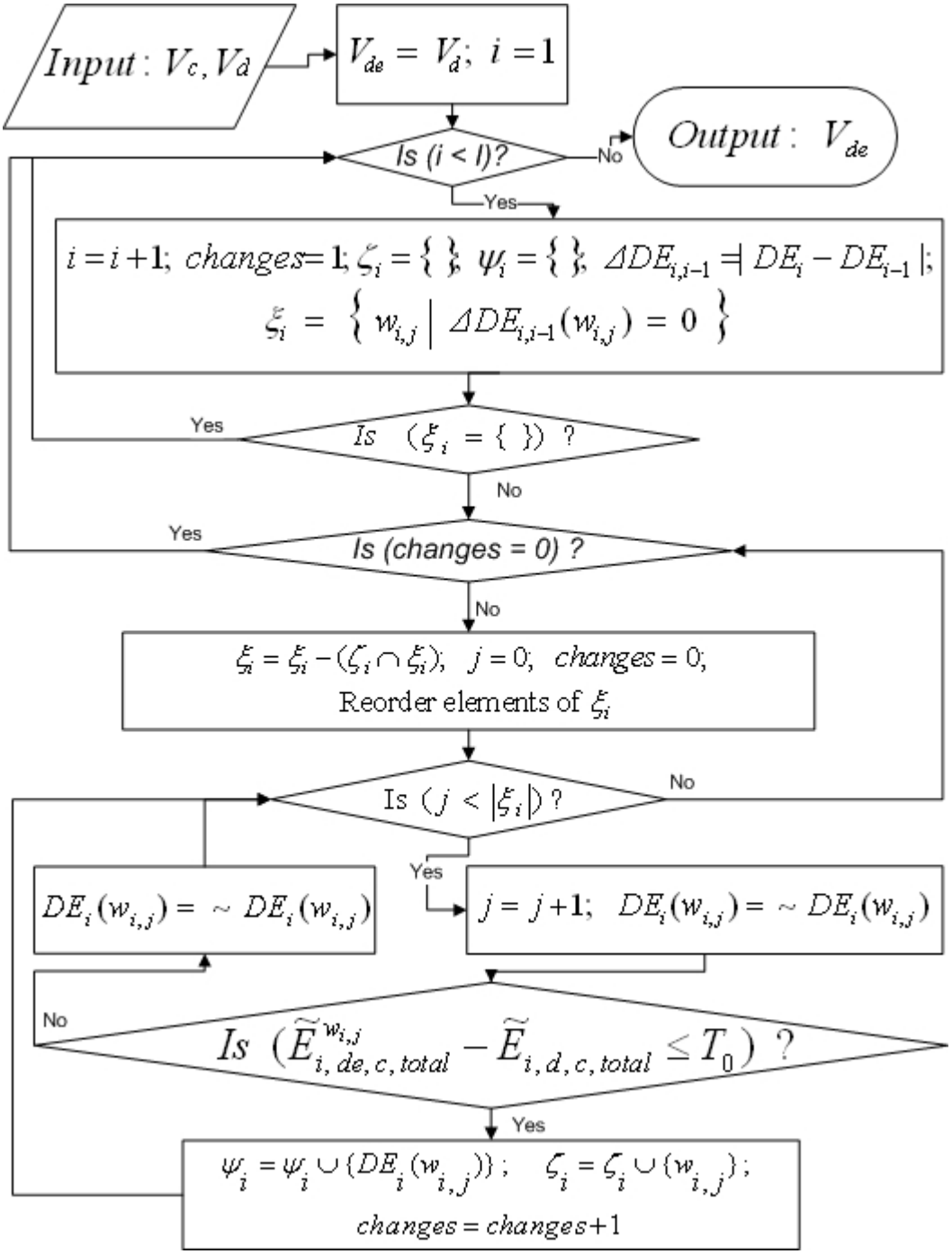

Fig. 1. Reducing DWE in a binary halftone video using Algorithm I.

the ordered set of pixel locations that have the same value between the current and the preceding halftone frames. The derivation explained in detail in [36] shows that $\Delta\widetilde{E}^{w_{i,1}}_{i,de,c,total}$ can be evaluated using $a_i(w_{i,1})$, c_{pp} and $c_{p\widetilde{E}_{i,de,c}}$ as:

$$\Delta\widetilde{E}^{w_{i,1}}_{i,de,c,total} = a_i^2(w_{i,1})c_{pp}(0) - 2a_i(w_{i,1})c_{p\widetilde{E}_{i,de,c}}(w_{i,1}) \tag{21}$$

The above expression is for $j = 1$. The evaluation of $\Delta\widetilde{E}^{w_{i,j}}_{i,de,c,total}$ for $j > 1$ is done similarly.

The correlation matrix c_{pp} is dependent on the HVS filter used, and thus stays the same for the entire video. Therefore, c_{pp} needs to be evaluated only once. The cross-correlation matrix $c_{p\widetilde{E}_{i,de,c}}$ must change everytime DE_i, and hence $\Delta\widetilde{E}^{w_{i,1}}_{i,de,c,total}$, changes. This happens whenever a *trial* change in DE_i is *accepted*. The initial matrix $c_{p\widetilde{E}_{i,de,c}}$ is calculated once per frame and, thereafter, only needs to be updated whenever a *trial* change in the enhanced frame DE_i is *accepted*. This updating operation has also been derived in [36], and, if a trial change has been accepted in DE_i at pixel location $w_{i,j}$, $c_{p\widetilde{E}_{i,de,c}}$ is updated using:

$$c_{p\widetilde{E}_{i,de,c}}(l) = c_{p\widetilde{E}_{i,de,c}}(l) - a_i(w_{i,j})c_{pp}(l - w_{i,j}) \qquad (22)$$

where $l = (m,n)^T$ denotes a pixel location in $c_{p\widetilde{E}_{i,de,c}}$.

Note that in the evaluation of $\Delta\widetilde{E}^{w_{i,j}}_{i,de,c,total}$, only scalar arithmetic is needed. Computational efficiency is, therefore, achieved by the algorithm described in this section.

Fig. 2 depicts the algorithm that achieves DWE reduction in a computationally efficient manner. As the processing of a frame begins, $\widetilde{E}_{i,de,c,total}$ is evaluated before making any changes. Note that at this point, $\widetilde{E}_{i,de,c,total}$ is equal to $\widetilde{E}_{i,d,c,total}$, since the initial DE_i is equal to D_i. This initial value of $\widetilde{E}_{i,de,c,total}$ is assigned to $\bar{E}_{i,de,c,total}$. Now, to evaluate the effect of any subsequent trial change (in pixel value of a location $w_{i,j}$ in the enhanced frame DE_i), ($\bar{E}_{i,de,c,total}$ + $\Delta\widetilde{E}^{w_{i,j}}_{i,de,c,total}$) is compared against ($\widetilde{E}_{i,d,c,total}$ + T_0). If ($\bar{E}_{i,de,c,total}$ + $\Delta\widetilde{E}^{w_{i,j}}_{i,de,c,total}$) is less than or equal to ($\widetilde{E}_{i,d,c,total}$ + T_0), then the trial change does not increase the perceptual error of DE_i by more than T_0 relative to the perceptual error of D_i. When this is so, the trial change is accepted. Otherwise, the trial change is rejected, and the pixel value is changed back to its original value. Similar to the algorithm of Section III-A, T_0 still controls the amount of (spatial) perceptual error introduced in frame DE_i during the process of DWE reduction. If the trial change is accepted, then $\bar{E}_{i,de,c,total}$ is updated as:

$$\bar{E}_{i,de,c,total} = \bar{E}_{i,de,c,total} + \Delta\widetilde{E}^{w_{i,j}}_{i,de,c,total} \qquad (23)$$

Note that the update suggested in (23) needs to be done everytime a pixel value is changed in the i^{th} enhanced frame, DE_i. This update ensures that, at any moment, $\bar{E}_{i,de,c,total}$ reflects the actual perceptual error of the enhanced frame DE_i due to all pixel changes that have taken place thus far. Note that doing so enables $\bar{E}_{i,de,c,total}$ to track the total perceptual error of the enhanced frame DE_i during the enhancement process. This enables the algorithm to decide whether to accept a trial change or not.

C. Algorithm III: Reduction of Dirty-window-effect under Spatial and Temporal Quality Constraints

The enhancement algorithms introduced in Sections III-A and III-B reduce DWE while attempting to constrain any resulting *additional* degradation in the spatial quality of the constituent frames of the halftone video that is being enhanced. In Section III-A, we briefly mentioned the possibility of the introduction of flicker, a temporal artifact, as a result of DWE reduction. Thus far, we have not talked about how introduction of flicker gets controlled in the process of reducing DWE in medium frame-rate binary video halftones. The DWE reduction results of Section III-B report any change in the Flicker Index, which is a measure of flicker [1]. Note that the reduction of DWE generally resulted in the introduction of flicker. The relationship between flicker and DWE has been discussed in detail in [1]. In this section, we discuss how flicker can be controlled besides controlling the frames' spatial quality in the process of DWE reduction.

The algorithms of Sections III-A and III-B constrain the introduction of additional spatial perceptual error using a threshold T_0. The control parameter T_0 also affects the introduction of flicker. A lower value of T_0 means fewer additional spatial artifacts, if any. A lower T_0 also means less reduction in DWE. Lesser reduction in DWE could generally mean lesser additional flicker in the enhanced video. Thus, T_0 has an impact on both spatial quality and flicker. Using T_0 to control the tradeoff between flicker and DWE is not the best way though. This is so because T_0 is also "tied" to the spatial quality of the frames of the halftone video.

We would like to introduce an additional parameter in the DWE reduction algorithm of this section to *separately* control flicker. Doing so will help "decouple" the control of temporal and spatial quality during the enhancement process. This might, for example, be desirable in situations where a lower spatial quality might be acceptable but a higher flicker is not. The control parameter T_0 does not explicitly specify the (spatial) regions where reducing DWE is more critical. The additional control parameter of this section is aimed to give us that capability. In doing so, the algorithm introduced in this section utilizes the temporal artifact assessment framework detailed in [1].

For the preceding two sections, ξ_i, as defined by (14), is the ordered set of pixel locations that have the same values between the two adjacent frames DE_i and DE_{i-1}. Recall that the elements of ξ_i are indexed by j with the j^{th} element of ξ_i denoted by $w_{i,j}$. For the algorithms of the preceding two sections (Figs. 1 and 2), all pixel locations belonging to ξ_i are candidates for a trial change. The development of the DWE assessment framework in [1], however, suggests that not all pixel locations belonging to ξ_i contribute to the perception of DWE equally. Therefore, we need not consider every pixel location belonging to ξ_i (as defined by (14)) for a trial change.

For the algorithm of this section, we modify the definition of ξ_i based on the DWE assessment framework of [1]. It was shown in [1] that a higher value of the product $(1-SSIM\{C_i, C_{i-1}\}(m,n))\cdot(1-W_i(m,n))$ meant that any pixels that have the same value at location (m,n) of successive halftone frames contribute more to the perception of DWE. Here $SSIM\{C_i, C_{i-1}\}$ refers to the Structural Similarity (SSIM) Index Map [38] evaluated between the continuous-tone frames C_i and C_{i-1} and scaled to have its pixels take values between 0 and 1 inclusive. Furthermore, W_i represents an image that has pixels with values approximating the local contrast content of the continuous-tone frame C_i [1].

Therefore, the pixels locations that should be trial changed in the enhanced frame DE_i can be determined by checking the value of the product $(1 - SSIM\{C_i, C_{i-1}\}(w_{i,j}))\cdot(1 - W_i(w_{i,j}))$. For this section, ξ_i is redefined as:

$$\xi_i = \{w_{i,j} : (DE_i(w_{i,j}) = DE_{i-1}(w_{i,j}))\} \cap \{w_{i,j} : (1 - SSIM\{C_i, C_{i-1}\}(w_{i,j}))\cdot(1 - W_i(w_{i,j})) > \tau_{dwe}\} \qquad (24)$$

where τ_{dwe} is a threshold that, besides the threshold T_0, controls the degree by which DWE gets reduced. τ_{dwe}, and

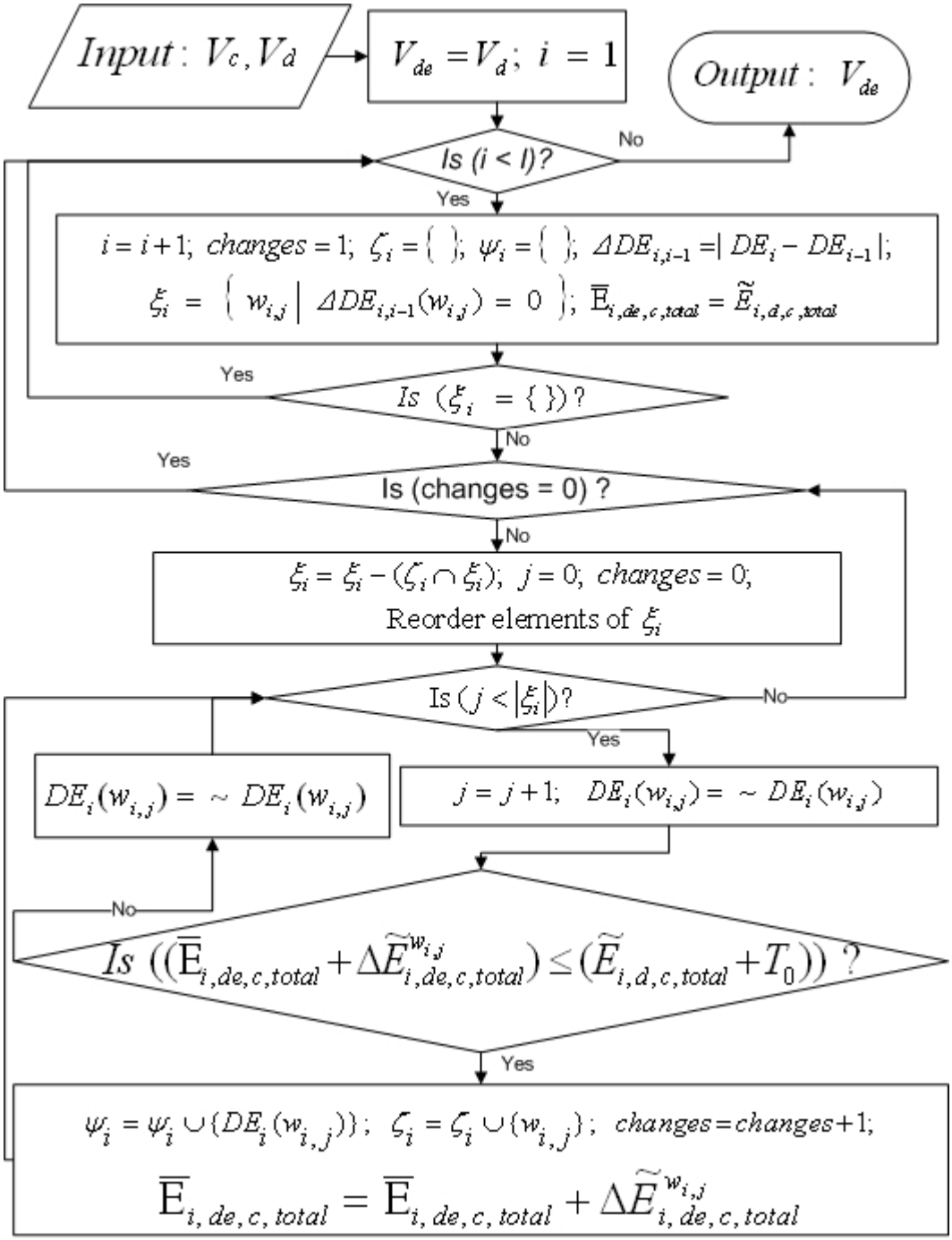

Fig. 2. Reducing DWE in a binary halftone video using Algorithm II. The algorithm depicted here is computationally more efficient than the algorithm depicted in Fig. 1. Algorithm III defines ξ_i differently, but otherwise is the same as algorithm II.

T_0 are the two parameters of the algorithm of this section. The value of T_0, as discussed earlier, mainly impacts the reduction of DWE, and the individual frame quality of the enhanced video V_{de}. τ_{dwe} determines the pixel locations where DWE needs to be reduced, and in the process, it controls the introduction of flicker. A lower value of τ_{dwe} means that possibly more pixels will be trial changed. This could possibly result in a lower DWE, if the trial changes are accepted. This could also result in higher flicker. Regardless of the value of τ_{dwe}, any degradation in the perceptual quality of individual frames of V_{de} is still controlled by T_0.

IV. Results

In this section, we present the results of reducing DWE in medium frame rate binary halftone videos using implementations based on the concepts depicted in Fig. 2. We first describe the results of video halftone enhancement using Algorithm II, and then the results obtained using Algorithm III. The original halftone videos and their enhanced versions can be viewed by

following the website link at [39]. If the provided link http://users.ece.utexas.edu/~bevans/papers/2012/videohalftoning/index.html does not work by a direct click on the link shown in the electronic version of this paper, please type the website address (link) directly in your browser.

The search space for a suitable pattern of binary pixels in a frame is finite. For each MxN binary frame, there can be 2^{MN} possible frames to choose from and the algorithms proposed in this paper converge. As discussed in Section III-A, there are different possibilities for convergence criterion used to determine whether the processing of a frame was complete. For generating the enhancement results presented here, convergence criterion was checked after *two* full scans of the frame (as opposed to the suggestion of one full scan in Fig. 2). The two successive scans, completed before checking convergence criterion, comprised of a horizontal and a vertical raster scan. Also, a trial change in the value of the pixel located at $w_{i,j}$ was accepted if ($\bar{E}_{i,de,c,total}$ + $\Delta\widetilde{E}^{w_{i,j}}_{i,de,c,total}$) was *less* than ($\widetilde{E}_{i,d,c,total}$ + T_0). For the initial threshold, a value of $T_0 = 0$ was used. The error metric, used to constrain the degradation of spatial quality of a frame, is dependent on the HVS filter implementation. Any filter used to represent the HVS is typically tuned to a particular application [35]. The tuning might require modification of the filter parameters to suit the needs of the display designer. We have used an HVS filter *based* on Nasanen's model [32] that has already been discussed in this paper. The parameter values used were $a = 131.6$, $b = 0.3188$, $c = 0.525$, $d = 3.91$, and $L = 400$. We used a filter support of 11x11 pixels and assumed a screen resolution of 94 pixels per inch, as well as a viewing distance of 12 inches.

Before attempting DWE reduction, some preprocessing was performed on the input halftone and continuous-tone videos. The continuous-tone video, V_c was pre-processed by performing an edge sharpening operation on each of its frames. The first frame of the halftone video, V_d, was improved using the DBS algorithm [40].

It was shown in [1], [22] that the frame-independent ordered dither (FIOD) method produces videos with excessive DWE. In the FIOD method, the first halftone sequence is formed by using ordered-dither technique on each frame independently [1]. For ordered-dither, the threshold array was formed by using a 32x32 void-and-cluster mask [41]. Since FIOD method produces halftones with excessive DWE, for halftone video enhancement, we demonstrate the results of enhancement done on the videos generated using FIOD.

Standard continuous-tone video sequences were used for testing at 30 frames per second (fps) [42]. The videos displayed at 15 fps were formed by halftoning a downsampled version of these continuous-tone sequences. These videos were halftoned using FIOD method, and were then enhanced by our algorithm. Table II describes the videos used.

Figs. 3 through 8 compare the performance of the videos generated using the FIOD algorithm with the videos enhanced using Algorithm II. The DWE performance is evaluated using the DWE Index, DWE, of [1]. The flicker performance is evaluated using the Flicker Index, F, of [1]. F and DWE can take values between 0 and 1 inclusive. A higher value of F means higher flicker. Similarly, a higher value of DWE means more DWE. In medium frame-rate binary halftone videos produced from grayscale continuous-tone videos, flicker and DWE are related [1]. Please refer to [1] for a more in-depth analysis of flicker and DWE in medium frame-rate binary halftone videos. To assess how well the enhancement algorithm preserves the spatial quality of the input halftone videos, a spatial quality assessment measure is needed. To assess the results, it is better to use a measure for spatial quality that was not utilized in the design of the algorithm. Therefore, a measure different than the spatial error measure used to enhance the videos is utilized.

TABLE II
DESCRIPTION OF 30 FPS AND 15 FPS VIDEOS.

Sequence	Frames (30 fps)	Frames (15 fps)	Spatial Resolution (in Pixels)
Caltrain	33	17	400x512
Tempete	150	75	240x352
Miss America	150	75	288x360
Susie	75	38	240x352
Tennis	150	75	240x352
Trevor	99	50	256x256
Garden	61	31	240x352
Salesman	449	225	288x360
Football	60	30	240x352

We use a spatial quality measure based on the Structural Similarity (SSIM) index [38]. It is a full-reference measure. As its name suggests, the SSIM index attempts to quantify the loss of structural information in the distorted image. We use the original mean SSIM index (MSSIM) [38] that can take values between -1 and 1 inclusive. The MSSIM index [38] gives a value for each frame. To get a single number for the entire video, we compute average of the MSSIM index for all the frames in the video.

Let us formalize this discussion. Let $S_i(C_i, D_i)$ denote a measure of spatial perceptual quality of the i^{th} halftone frame D_i with respect to the continuous-tone frame C_i. Let $S(V_c, V_d)$ represent the Spatial Quality Index of the halftone video V_d with respect to the continuous-tone video V_c. The Spatial Quality Index $S(V_c, V_d)$ for the halftone video with a total of I frames is then:

$$S(V_c, V_d) = \frac{\sum_i S_i(C_i, D_i)}{I} \text{ for } i > 0 \qquad (25)$$

We set $S_i(C_i, D_i)$ equal to MSSIM(C_i,D_i) of [38]. For F, and DWE, a *lower* value indicates better performance. However, a *lower* value of S indicates worse spatial quality.

The results of our implementation are shown in Figs. 3, 4, 5, 6, 7, and 8. In the bar charts of Figs. 3 and 6, note the considerable improvement in DWE performance, as shown by a lower value of the DWE Index, DWE. However, considerable flicker has also been introduced as shown by an increase in the Flicker Index, F in Figs. 4 and 7. It can be seen in Figs. 5 and 8 that the value of spatial quality measure S for the original and the enhanced halftone videos is generally fairly close indicating that the spatial quality of

the halftone videos is not reduced by much, if at all, using our implementation of the enhancement algorithm.

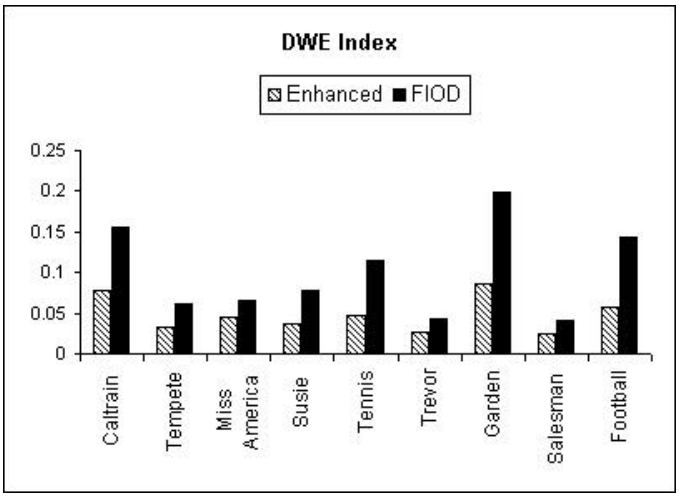

Fig. 3. The DWE Index, DWE [1], for 30 fps FIOD and enhanced halftone videos. A *lower* value of DWE indicates *better* performance. Halftone videos were enhanced using Algorithm II (Section III-B). Note the reduction of DWE in the enhanced videos.

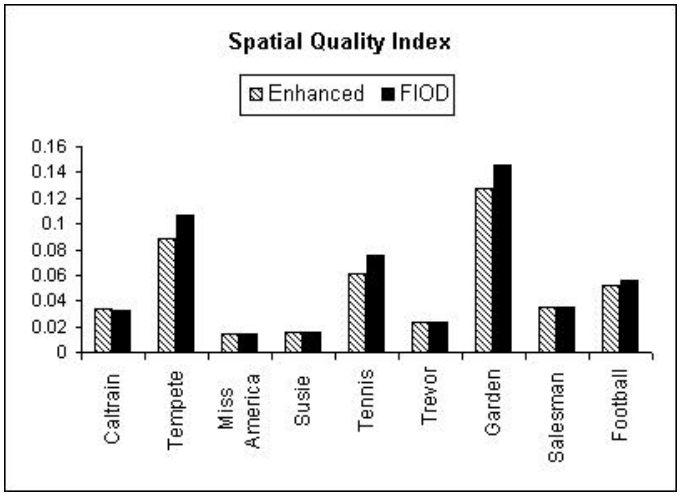

Fig. 5. The Spatial Quality Index, S (based on [38]), for 30 fps FIOD and enhanced halftone videos. Halftone videos were enhanced using Algorithm II (Section III-B). A *higher* value of S indicates *better* performance. Note the spatial quality stays relatively unaffected in the enhanced videos.

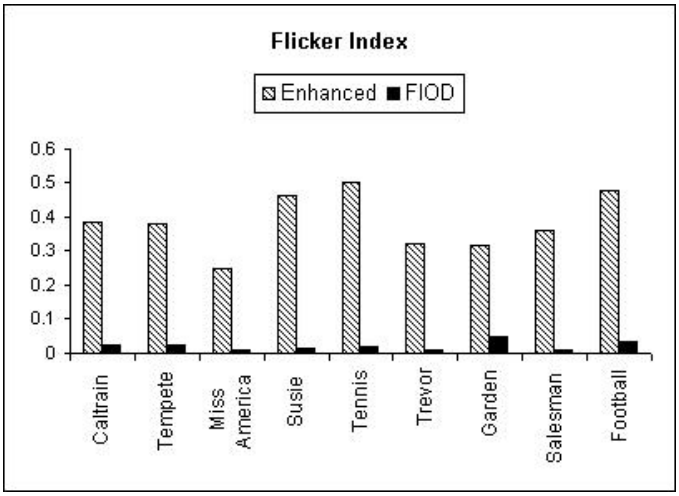

Fig. 4. The Flicker Index, F [1], for 30 fps FIOD and enhanced halftone videos. A *lower* value of F indicates *better* performance. Halftone videos were enhanced using Algorithm II (Section III-B). Note the flicker increase in the enhanced videos.

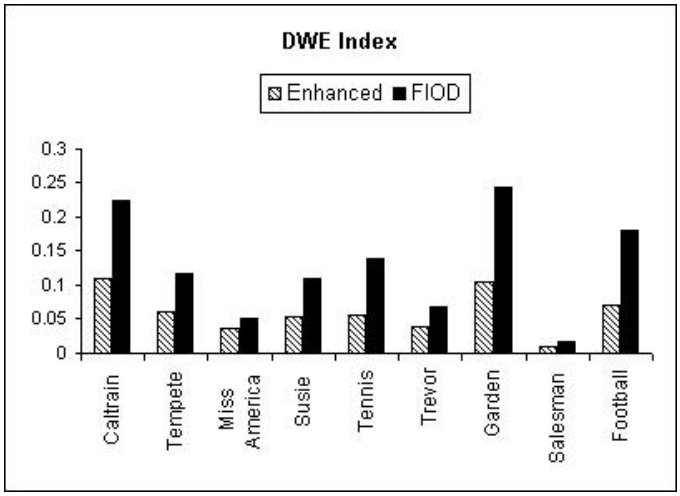

Fig. 6. The DWE Index, DWE [1], for 15 fps FIOD and enhanced halftone videos. A *lower* value of DWE indicates *better* performance. Halftone videos were enhanced using Algorithm II (Section III-B). Note the reduction of DWE in the enhanced videos.

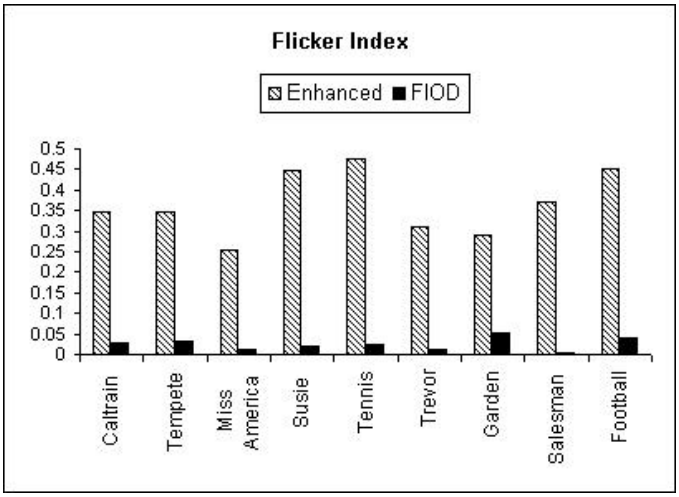

Fig. 7. The Flicker Index, F [1], for 15 fps FIOD and enhanced halftone videos. A *lower* value of F indicates *better* performance. Halftone videos were enhanced using Algorithm II (Section III-B). Note the flicker increase in the enhanced videos.

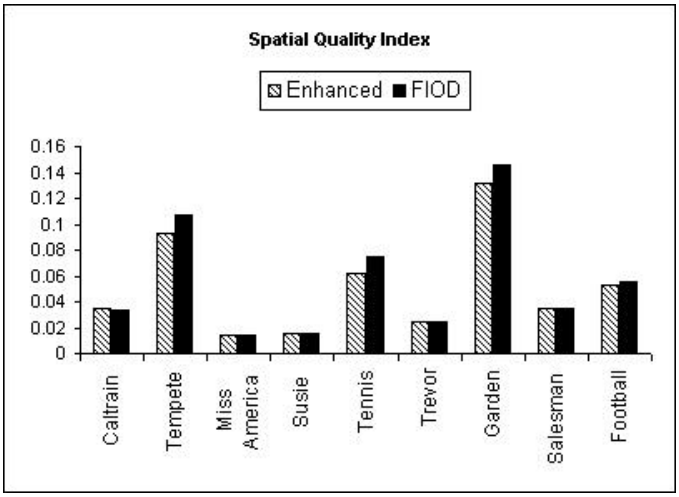

Fig. 8. The Spatial Quality Index, S (based on [38]), for 15 fps FIOD and enhanced halftone videos. Halftone videos were enhanced using Algorithm II (Section III-B). A *higher* value of S indicates *better* performance. Note the spatial quality stays relatively unaffected in the enhanced videos.

Next, we present the results of reducing DWE under spatial and temporal quality constraints using Algorithm III. The enhancement algorithm implementation used for producing these results is *based* on the DWE reduction concepts discussed in Section III-C. The general flow of algorithm implementation is *based* on Fig. 2 but with ξ_i defined by (24).

We report the results on 30 fps using Figs. 9, 10, and 11. Figs. 12, 13, and 14 depict the enhancement performance for 15 fps videos. For the results reported in this paper, $\tau_{dwe} = 0.1$. Note that the spatial quality of the two (input and enhanced) videos is fairly close for the tested sequences. Compare these results with the results reported depicted in the bar charts of Figs. 3 through 8 to note that while there is less reduction in DWE in halftones enhanced using the modified algorithm of Section III-C, the increase in flicker is smaller than the increase observed in Figs. 4 and 7. This is what was expected of the enhancement algorithm modification proposed in Section III-C. The additional (control) parameter τ_{dwe} is used to provide a balance between DWE and flicker performance of the enhanced video. The results shown in Figs. 9, 10, 12, and 13 confirm this.

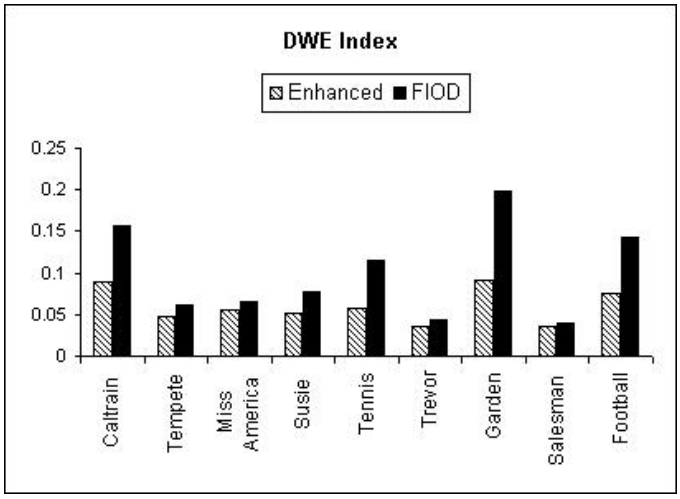

Fig. 9. The DWE Index, DWE [1], for 30 fps FIOD and enhanced halftone videos. A *lower* value of DWE indicates *better* performance. Halftone videos were enhanced using Algorithm III (Section III-C). Note the reduction of DWE in the enhanced videos.

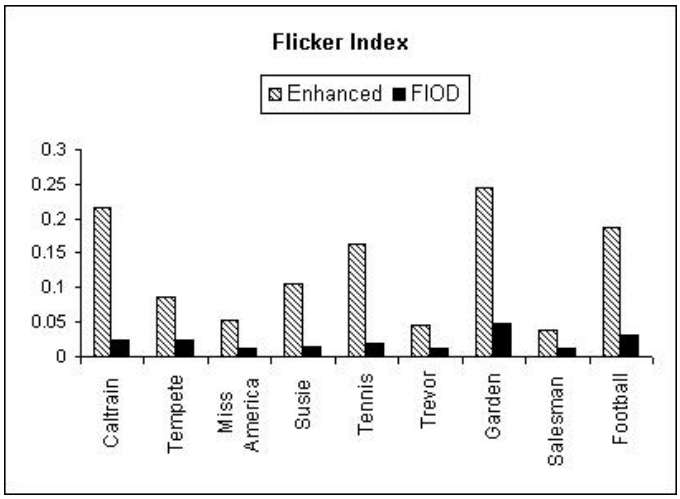

Fig. 10. The Flicker Index, F [1], for 30 fps FIOD and enhanced halftone videos. A *lower* value of F indicates *better* performance. Halftone videos were enhanced using Algorithm III (Section III-C). Compared to Fig. 4, note the relatively lower increase in flicker of the enhanced videos.

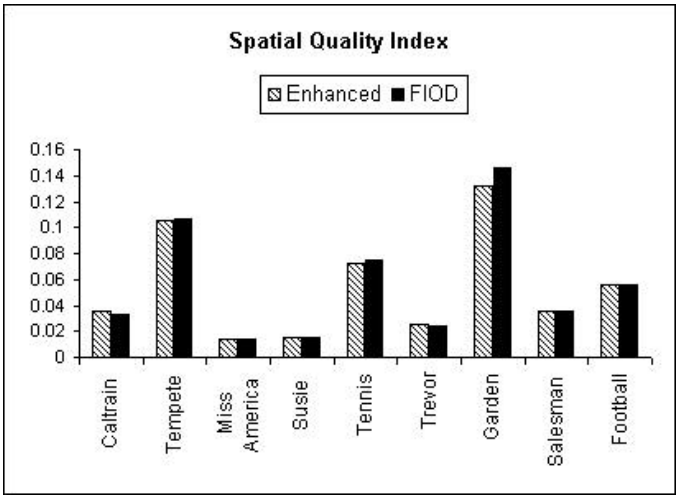

Fig. 11. The Spatial Quality Index, S (based on [38]), for 30 fps FIOD and enhanced halftone videos. Halftone videos were enhanced using Algorithm III (Section III-C). A *higher* value of S indicates *better* performance. Note the spatial quality stays relatively unaffected in the enhanced videos.

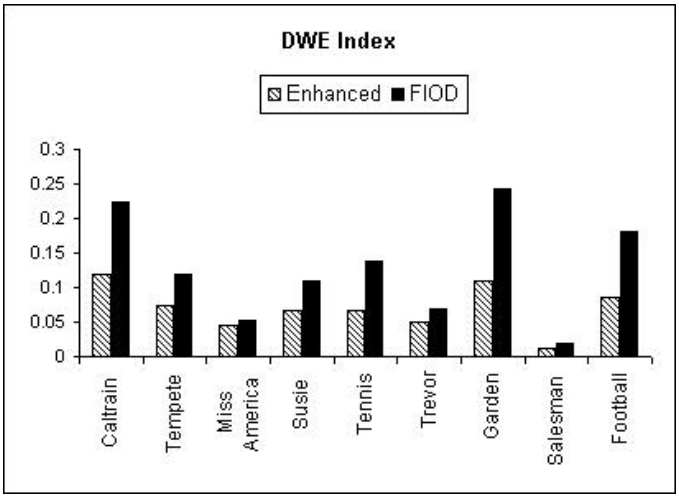

Fig. 12. The DWE Index, DWE [1], for 15 fps FIOD and enhanced halftone videos. A *lower* value of DWE indicates *better* performance. Halftone videos were enhanced using Algorithm III (Section III-C). Note the reduction of DWE in the enhanced videos.

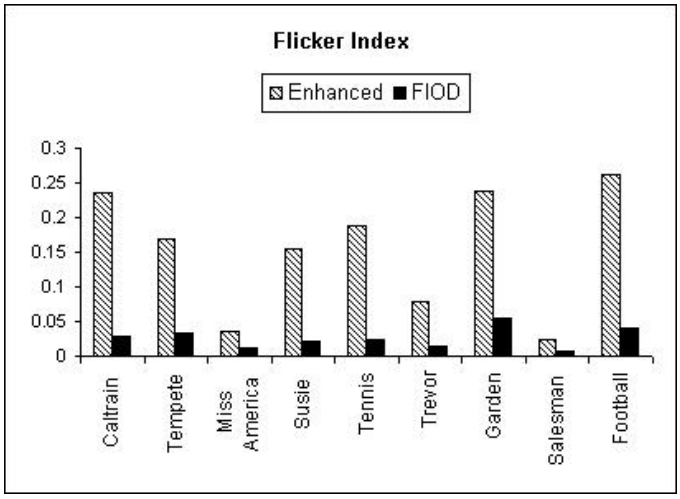

Fig. 13. The Flicker Index, F [1], for 15 fps FIOD and enhanced halftone videos. A *lower* value of F indicates *better* performance. Halftone videos were enhanced using Algorithm III (Section III-C). Compared to Fig. 7, note the relatively lower increase in flicker of the enhanced videos.

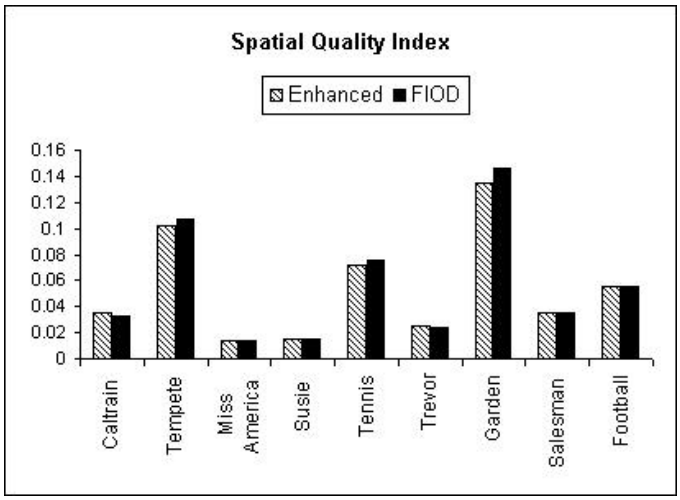

Fig. 14. The Spatial Quality Index, S (based on [38]), for 15 fps FIOD and enhanced halftone videos. Halftone videos were enhanced using Algorithm III (Section III-C). A *higher* value of S indicates *better* performance. Note the spatial quality stays relatively unaffected in the enhanced videos.

V. Flicker and DWE performance of some other Halftone Generation Methods

The primary goal of the algorithms proposed in this paper is to reduce DWE. Thus far we have shown how that is done by reducing DWE in FIOD halftone videos. Now we present the flicker and DWE performance of halftone videos generated using four video halftone generation methods [1], [3], [22], [43]. The video halftone generation methods used to generate the videos discussed in this section include Gotsman's method (GM) [3], Modified Gotsman's method (MGM) [1], [22], Frame-independent Floyd-Steinberg error diffusion (FIFSED) [43], and Frame-dependent Floyd-Steinberg error diffusion (FDFSED) [1], [22]. In this section, we also provide more enhancement results obtained by reducing DWE in 30 fps videos that were originally generated using GM [3].

Figs. 15 and 16 show the flicker and DWE performance of 30 fps halftone videos generated using GM, MGM, FIFSED, and FDFSED algorithms. Figs. 17 and 18 show the flicker and DWE performance of 15 fps halftone videos generated using GM, MGM, FIFSED, and FDFSED. The purpose of the results reported in these figures is to give the audience an opportunity to see how FIOD and the enhancement methods of Section III compare with some other methods in terms of flicker and DWE performance. This comparison can also facilitate the choice of a video halftone generation algorithm or an enhancement algorithm for any particular application/device.

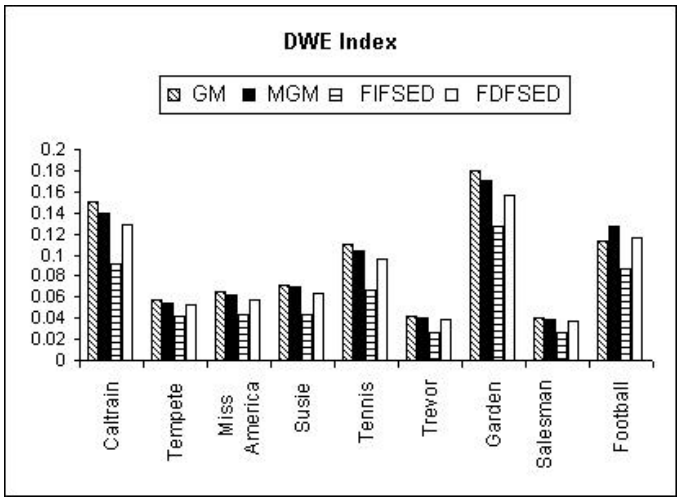

Fig. 15. The DWE Index, DWE [1], for 30 fps GM [3], MGM [1], FIFSED [43], and FDFSED [1] halftone videos. A *lower* value of DWE indicates *better* performance.

The algorithms proposed in this paper are suitable for enhancing videos that suffer from excessive DWE. Note in Figs. 15, 16, 17, and 18 that videos generated using FIFSED suffer from minimal DWE. These videos (generated using FIFSED) are an example of videos that do not require DWE enhancement, and thus will not benefit (much) from enhancement using the proposed techniques of this paper. In the previous section, we have presented the results of reducing DWE in halftone videos produced using FIOD. In general, as can be seen from the flicker and DWE data presented thus far, FIOD produces excessive DWE. To serve as another example of DWE reduction using our proposed methods, we now demonstrate the results of reducing DWE in 30 fps video halftones originally produced using GM [3]. The halftone videos generated using GM [3] and the enhanced halftone videos can be viewed at [39]. We first use Algorithm II (Section III-B). Figs. 19, 20, and 21 show the results of enhancing the halftone videos produced using GM. In Fig. 19, note the significant reduction in DWE. As you would expect, in Fig. 20, note the resulting increase in flicker. Since the spatial quality of each halftone frame was attempted to be preserved in Algorithm II, observe in Fig. 21 that the spatial quality is relatively unaffected.

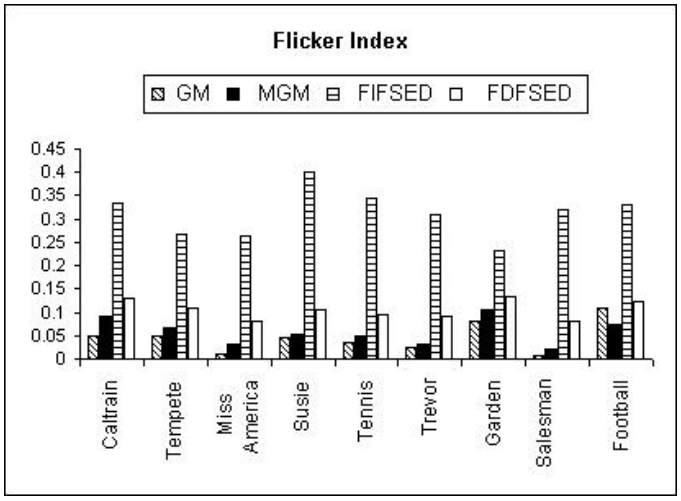

Fig. 16. The Flicker Index, F [1], for 30 fps GM [3], MGM [1], FIFSED [43], and FDFSED [1] halftone videos. A *lower* value of F indicates *better* performance.

Figs. 22, 23, and 24 show the results of the enhancement of GM halftone videos using Algorithm III (Section III-C). In Fig. 22, note the reduction in DWE. Note that the reduction in DWE is not as much as achieved using Algorithm II (Fig. 19). Nevertheless, the reduction in DWE is still quite remarkable. On the other hand, in Fig. 23, note the resulting increase in flicker is smaller than that observed using Algorithm II (Fig. 20). Finally, since Algorithm III also attempts to prevent reduction in the spatial quality of each halftone frame, observe in Fig. 24 that the spatial quality is relatively unaffected.

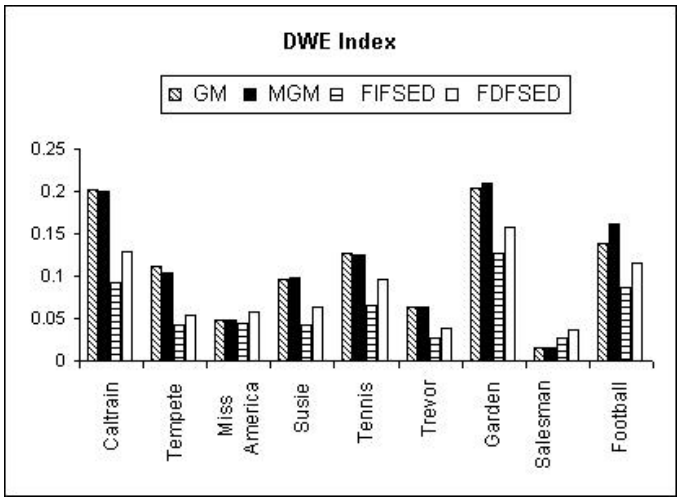

Fig. 17. The DWE Index, DWE [1], for 15 fps GM [3], MGM [1], FIFSED [43], and FDFSED [1] halftone videos. A *lower* value of DWE indicates *better* performance.

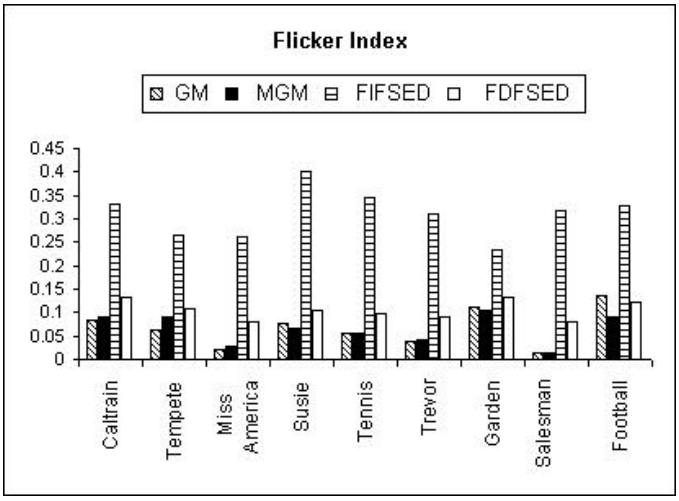

Fig. 18. The Flicker Index, F [1], for 15 fps GM [3], MGM [1], FIFSED [43], and FDFSED [1] halftone videos. A *lower* value of F indicates *better* performance.

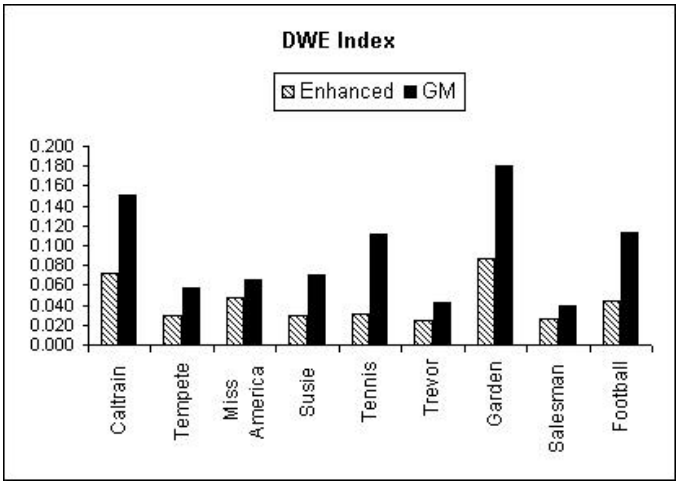

Fig. 19. The DWE Index, DWE [1], for 30 fps GM [3] and enhanced halftone videos. A *lower* value of DWE indicates *better* performance. Halftone videos were enhanced using Algorithm II (Section III-B). Note the reduction of DWE in the enhanced videos.

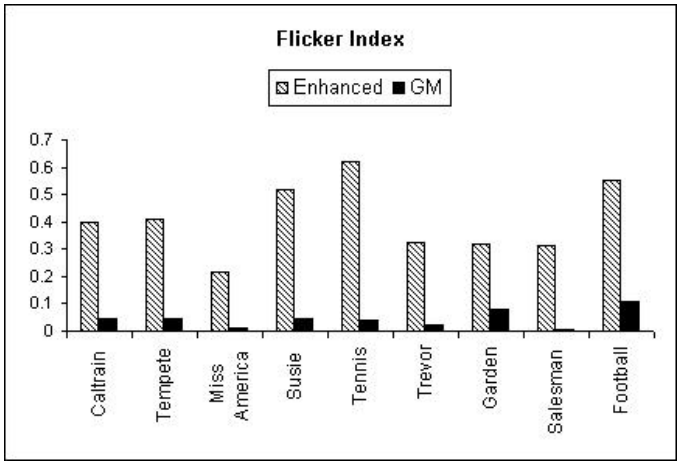

Fig. 20. The Flicker Index, F [1], for 30 fps GM [3] and enhanced halftone videos. A *lower* value of F indicates *better* performance. Halftone videos were enhanced using Algorithm II (Section III-B). Note the flicker increase in the enhanced videos.

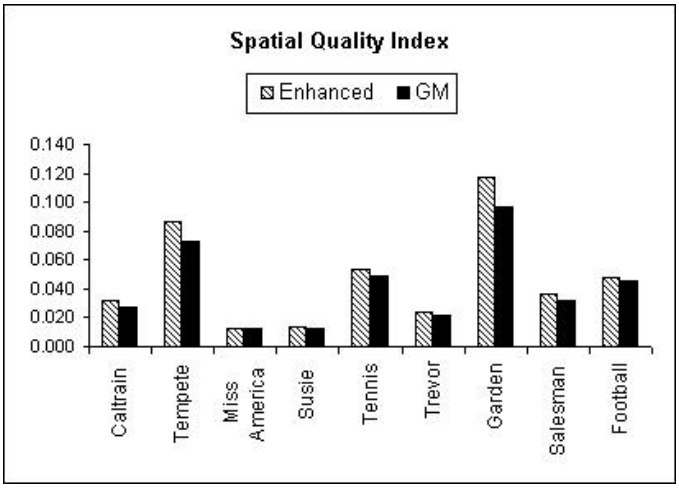

Fig. 21. The Spatial Quality Index, S (based on [38]), for 30 fps GM [3] and enhanced halftone videos. Halftone videos were enhanced using Algorithm II (Section III-B). A *higher* value of S indicates *better* performance.

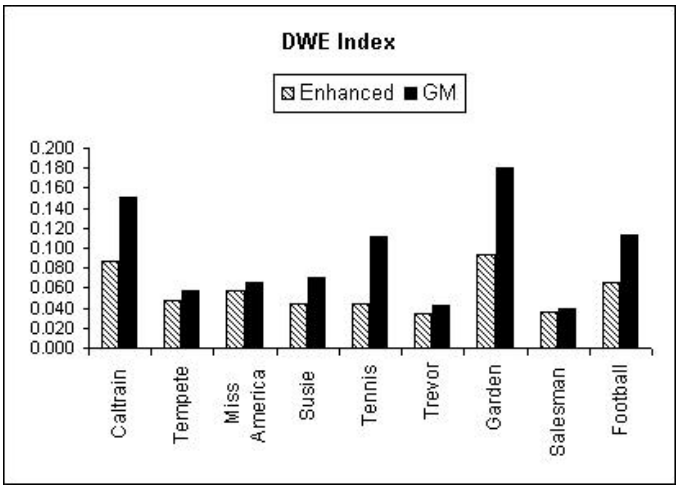

Fig. 22. The DWE Index, DWE [1], for 30 fps GM [3] and enhanced halftone videos. A *lower* value of DWE indicates *better* performance. Halftone videos were enhanced using Algorithm III (Section III-C). Note the reduction of DWE in the enhanced videos.

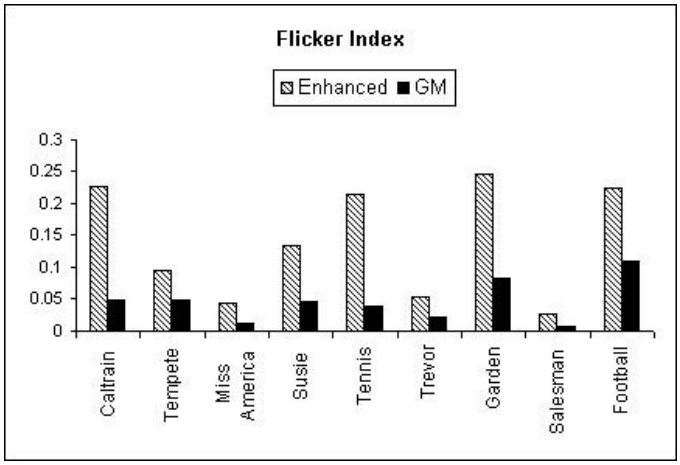

Fig. 23. The Flicker Index, F [1], for 30 fps GM [3] and enhanced halftone videos. A *lower* value of F indicates *better* performance. Halftone videos were enhanced using Algorithm III (Section III-C). Note the flicker increase in the enhanced videos.

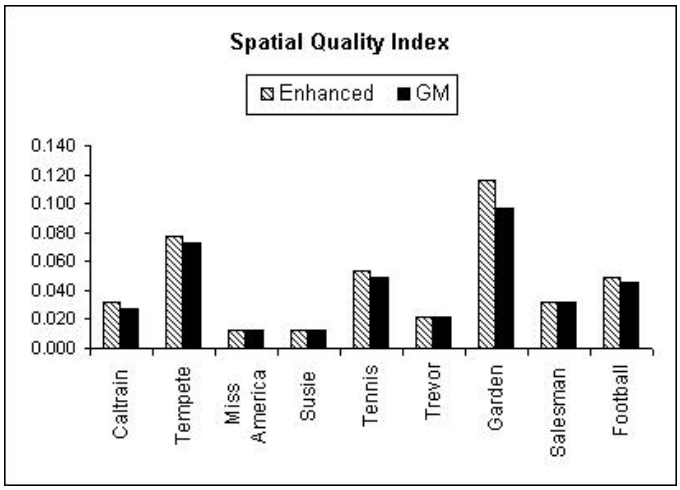

Fig. 24. The Spatial Quality Index, S (based on [38]), for 30 fps GM [3] and enhanced halftone videos. Halftone videos were enhanced using Algorithm III (Section III-C). A *higher* value of S indicates *better* performance.

VI. Conclusion

This paper proposes three algorithms for DWE reduction in medium frame-rate binary video halftones. The first two algorithms reduce DWE under a spatial quality constraint. The third algorithm reduces DWE under both spatial and temporal quality constraints. Results of reducing DWE using two algorithms are presented and compared. The results depict a reduction in DWE. This paper also presents the flicker and DWE performance of several video halftone generation algorithms.

The algorithms proposed in this paper potentially improve the DWE performance of a halftone video. This was done using a relatively simpler HVS model. Based on the contributions of this paper, several research avenues could be explored. A potential future contribution could be to compare the performance of the proposed algorithms using different and possibly more sophisticated models of the HVS. Another related contribution could be to analyze the trade-off between computational complexity and the sophistication of the HVS model used.

References

[1] H. Rehman and B. L. Evans, "A framework for the assessment of temporal artifacts in medium frame-rate binary video halftones," *EURASIP Journal on Image and Video Processing*, vol. 2010, Oct. 2010.

[2] D. P. Hilgenberg, T. J. Flohr, C. B. Atkins, J. P. Allebach, and C. A. Bouman, "Least-squares model-based video halftoning," *Human Vision, Visual Processing, and Digital Display V*, vol. 2179, no. 1, pp. 207–217, 1994.

[3] C. Gotsman, "Halftoning of image sequences," *The Visual Computer*, vol. 9, no. 5, pp. 255–266, 1993.

[4] C. Hsu, C. Lu, and S. Pei, "Video halftoning preserving temporal consistency," in *Proc. IEEE Int. Conf. on Multimedia and Expo*, 2007, pp. 1938–1941.

[5] H. Hild and M. Pins, "A 3-d error diffusion dither algorithm for halftone animation on bitmap screens," in *State-of-the-Art in Computer Animation*. Berlin, Germany: Springer-Verlag, 1989, p. 181190.

[6] Z. Sun, "Video halftoning," *IEEE Trans. on Image Processing*, vol. 15, no. 3, pp. 678–686, 2006.

[7] J. B. Mulligan, "Methods for spatiotemporal dithering," in *Proc. SID Int. Symp., Dig. Tech. Papers*, Seattle, WA, 1993, pp. 155–158.

[8] F. Cittadini, M. Remita, J. Pervillé, S. Berche, M. Chouikha, H. Brettel, and G. Alquié, "Contribution to quality assessment of digital halftoning algorithms," in *Color Imaging XII: Processing, Hardcopy, and Applications*, R. Eschbach and G. G. Marcu, Eds., vol. 6493, no. 1. SPIE, 2007, p. 64931D.

[9] R. A. Ulichney, *Digital Halftoning*. Cambridge, MA: MIT Press, 1987.

[10] D. L. Lau and G. R. Arce, *Modern Digital Halftoning*. CRC Press, 2008.

[11] T.-C. Chang and J. P. Allebach, "A new framework for characterization of halftone textures," *IEEE Transactions on Image Processing*, vol. 15, no. 5, pp. 1285–1299, May 2006.

[12] D. L. Lau, R. Ulichney, and G. R. Arce, "Blue- and green-noise halftoning models," *IEEE Signal Processing Magazine*, vol. 20, no. 4, pp. 28–38, July 2003.

[13] S. Hocevar and G. Niger, "Reinstating Floyd-Steinberg: Improved Metrics for Quality Assessment of Error Diffusion Algorithms," in *Lecture Notes in Computer Science*, vol. 5099. Springer, 2008, pp. 38–45.

[14] P.-E. Axelson, "Quality measures of halftoned images (a review)," Master's thesis, Department of Science and Technology, Link'oping University, Sweden, 2003.

[15] F. Nilsson, "Objective quality measures for halftoned images," *Journal of Optical Society of America*, vol. 16, no. 9, pp. 2151–2162, 1999.

[16] M. Pedersen, F. Albregtsen, and J. Y. Hardeberg, "Detection of worms in error diffusion halftoning," in *Image Quality and System Performance VI*, vol. 7242, no. 1. SPIE, 2009, p. 72420L.

[17] X. Wan, D. Xie, and J. Xu, "Quality evaluation of the halftone by halftoning algorithm-based methods and adaptive method," in *Image Quality and System Performance IV*, vol. 6494, no. 1. SPIE, 2007, p. 64940U.

[18] Q. Lin, "Halftone image quality analysis based on a human vision model," in *Human Vision, Visual Processing, and Digital Display IV*, vol. 1913, no. 1. SPIE, 1993, pp. 378–389.

[19] H. Fang and X. Lu, "Characterization of error diffusion halftone images based on subband decompostion," in *IEEE Workshop on Multimedia Signal Processing*, Nov. 2005, pp. 1–4.

[20] T. D. Kite, B. L. Evans, and A. C. Bovik, "Modeling and quality assessment of halftoning by error diffusion," *IEEE Transactions on Image Processing*, vol. 9, no. 5, pp. 909–922, 2000.

[21] H. Rehman and B. L. Evans, "Flicker assessment of low-to-medium frame-rate binary video halftones," in *Proc. IEEE Southwest Symposium on Image Analysis and Interpretation*, May 2010.

[22] H. Rehman, "Artifact assessment, generation, and enhancement of video halftones," Ph. D., Department of Electrical and Computer Engineering, The University of Texas at Austin, USA, 2010.

[23] J. Sullivan, L. Ray, and R. Miller, "Design of minimum visual modulation halftone patterns," *IEEE Transactions on Systems, Man and Cybernetics*, vol. 21, no. 1, pp. 33 –38, jan/feb 1991.

[24] B. Kolpatzik and C. Bouman, "Optimized error diffusion for high quality image display," *Journal of Electronic Imaging*, vol. 1, no. 3, pp. 277–292, 1992.

[25] T. N. Pappas and D. L. Neuhoff, "Least-squares model-based halftoning," *IEEE Transactions on Image Processing*, vol. 8, no. 8, pp. 1102–1116, 1999.

[26] D. L. Neuhoff, T. N. Pappas, and N. Seshadri, "One-dimensional least-squares model-based halftoning," *Journal of the Optical Society of America*, vol. 14, no. 8, pp. 1707–1723, 1997.

[27] J. Sullivan, R. Miller, and G. Pios, "Image halftoning using a visual model in error diffusion," *Journal of the Optical Society of America*, vol. 10, no. 8, pp. 1714–1723, 1993.

[28] T. Mitsa and K. Varkur, "Evaluation of contrast sensitivity functions for the formulation of quality measures incorporated in halftoning algorithms," in *IEEE International Conference on Acoustics, Speech, and Signal Processing*, vol. 5, 27-30 1993, pp. 301 –304.

[29] A. Agar and J. P. Allebach, "Model-based color halftoning using direct binary search," *IEEE Transactions on Image Processing*, vol. 14, no. 12, pp. 1945 –1959, dec. 2005.

[30] F. W. Campbell, R. H. S. Carpenter, and J. Z. Levinson, "Visibility of aperiodic patterns compared with that of sinusoidal gratings," *The Journal of Physiology*, vol. 204, no. 2, p. 283, 1969.

[31] J. Mannos and D. Sakrison, "The effects of a visual fidelity criterion of the encoding of images," *IEEE Transactions on Information Theory*, vol. 20, no. 4, pp. 525–536, 1974.

[32] R. Nasanen, "Visibility of halftone dot textures," *IEEE transactions on systems, man, and cybernetics*, vol. 14, no. 6, pp. 920–924, 1984.

[33] S. Daly, "Subroutine for the generation of a two dimensional human visual contrast sensitivity function," Eastman Kodak, Tech. Rep. Tech. Rep. 233203y, 1987.

[34] H. K. Sang and J. P. Allebach, "Impact of HVS models on model-based halftoning," *IEEE Transactions on Image Processing*, vol. 11, no. 3, pp. 258–269, 2002.

[35] T. N. Pappas, J. P. Allebach, and D. L. Neuhoff, "Model-based digital halftoning," *IEEE Signal Processing Magazine*, vol. 20, no. 4, pp. 14–27, July 2003.

[36] D. J. Lieberman and J. P. Allebach, "A dual interpretation for direct binary search and its implicationsfor tone reproduction and texture quality," *IEEE Transactions on Image Processing*, vol. 9, no. 11, pp. 1950–1963, 2000.

[37] M. Analoui and J. P. Allebach, "Model-based halftoning using direct binary search," in *Proceedings of SPIE*, vol. 1666, 1992, p. 96.

[38] Z. Wang, A. C. Bovik, H. R. Sheikh, and E. P. Simoncelli, "Image quality assessment: from error visibility to structural similarity," *IEEE Transactions on Image Processing*, vol. 13, no. 4, pp. 600–612, 2004.

[39] H. Rehman and B. L. Evans. Video halftoning demo page. [Online]. Available: http://users.ece.utexas.edu/~bevans/papers/2012/videohalftoning/index.html

[40] D. J. Lieberman and J. P. Allebach, "Efficient model based halftoning using direct binary search," in *Proceedings of the IEEE International Conference on Image Processing*, 1997, pp. 775–778.

[41] R. A. Ulichney, "Void-and-cluster method for dither array generation," in *IS&T/SPIE Symposium on Electronic Imaging Science & Technology*, vol. 1913, no. 1. SPIE, 1993, pp. 332–343.

[42] R. P. I. Center for Image Processing Research. [Online]. Available: http://www.cipr.rpi.edu/resource/sequences/index.html

[43] R. Floyd and L. Steinberg, "An adaptive algorithm for spatial grayscale," in *Proc. SID Int. Symp., Dig. Tech. Papers*, 1976, p. 3637.

Hamood-Ur Rehman received the B.S.E.E., M.S.E. and Ph.D. degrees from The University of Texas at Austin, Austin, Texas, USA. His current research interests include digital image and video halftoning, image and video quality assessment, and digital image and video transmission and display.

Brian L. Evans is the Engineering Foundation Professor of Electrical and Computer Engineering at UT Austin. He earned his BSEECS (1987) degree from the Rose-Hulman Institute of Technology, and his MSEE (1988) and PhDEE (1993) degrees from the Georgia Institute of Technology. From 1993 to 1996, he was a post-doctoral researcher at the University of California, Berkeley.

Prof. Evans seeks to bridge gaps between signal processing theory and embedded real-time implementation for digital communications and digital image/video processing applications. His current research includes interference mitigation algorithms for communication systems, video display algorithms for cell phones, and design automation tools for multicore embedded systems.

Prof. Evans has published 200+ refereed conference and journal papers, and graduated 20 PhD students. In 2008, he was awarded the ECE Lepley Memorial Teaching Award. In 2011, he was awarded the university-wide Texas Exes Teaching Award. He received a 1997 US National Science Foundation CAREER Award.